

Modal analysis of frame structures with semi-rigid joints and viscoelastic connections modeled by fractional derivatives

Z. M. PAWLAK, M. ŁASECKA-PLURA, M. ŻAK-SAWIAK

*Faculty of Civil and Transport Engineering, Poznan University of Technology, Poland,
e-mails: zdzislaw.pawlak@put.poznan.pl, magdalena.lasecka-plura@put.poznan.pl,
martyna.zak-sawiak@put.poznan.pl*

THE PAPER PRESENTS TWO METHODS OF SOLVING the problem of the dynamics of a frame structure with viscoelastic bonds in nodes. In the first approach, known from the literature, two-node beam elements with three degrees of freedom in each node were used. Exact shape functions were adopted to obtain a stiffness matrix, a consistent mass matrix and a damping matrix for the beam element. These matrices were then modified by introducing rotational viscoelastic constraints at the boundary nodes. In the second approach, a new method of modelling viscoelastic bonds in frame structures was proposed. It consists in removing rigid bonds between elements along selected degrees of freedom and replacing them with a new, additional element with viscoelastic properties. This approach allows the use of any rheological model to describe viscoelastic bonds (i.e. an additional element) without the need to create a new modified finite element. In this work, an advanced rheological model, i.e. the fractional Kelvin model, was used to describe rotational viscoelastic bonds. The use of fractional derivatives to describe the damping properties reduces the number of parameters needed in the model, but leads to a non-linear eigenproblem. In order to solve the eigenvalue problem, the continuation method was used, and the dynamic characteristics of the structure were determined on the basis of the calculated eigenvalues. Selected structures with viscoelastic nodes were analyzed and the obtained results confirm the effectiveness of the proposed approach.

Key words: viscoelastic connections, rotational damping, rheological fractional model, dynamic characteristics of structure, modified finite element.



Copyright © 2023 The Authors.

Published by IPPT PAN. This is an open access article under the Creative Commons Attribution License CC BY 4.0 (<https://creativecommons.org/licenses/by/4.0/>).

1. Introduction

IN ENGINEERING PRACTICE, THE PROBLEM OF SEMI-RIGID CONNECTIONS is well recognized. Commercially available frame design programs usually have the feature to define purely pinned, fully rigid or semi-rigid connections with a limited elasticity. The elasticity of connections in frame structures has a significant impact on the static and dynamic response of the entire structure, therefore, this issue is the subject of many studies.

In the past, several studies have been conducted on analytical solutions for steel beams and frames with semi-rigid connections. However, many of these studies focused on the economic advantage of semi-rigid joints over perfectly rigid connections [1, 2].

In some papers, it is proposed to perform calculations for the static analysis of steel frames with semi-rigid connections using the rotational stiffness function of the connection [3, 4]. In order to take into account the influence of connections on the behavior of steel frames in [5] a mechanical model of node was developed based on the analogy to three springs and a non-deformable element. For such a model, the stiffness matrix and the nodal load vector of the beam element under bending were derived.

In the research on semi-rigid joints, much attention has been paid to the modeling of the moment-rotation relationship for various types of connections, also in recent years. In [6], connections of steel girders with the use of a shear tab welded to the supporting element and the beam web were analyzed. The authors proposed a method to predict the stiffness of such joints. In [7], the model of welded steel connection is presented as a 4-node finite element with 12 degrees of freedom. In [8] a model of a bolted connection of a beam with a column was examined with geometrical, material and contact nonlinearities. The obtained results were validated by the experimental results.

Much attention has been also paid to the issues of flexibility of connection and critical load of frames. In [5], it was shown that the flexibility of the joints has a significant impact on the elastic buckling load.

SIMÕES [9] and TRUONG *et al.* [10] concern the methods of optimal design of steel structures with semi-rigid joints. In [11], an analytical model was presented showing the interaction of the axial force and the bending moment and it was verified using experimental data. In [12] the experimental results supported by the finite element method analyses were used to develop a connection failure mechanism.

Steel frames with semi-rigid connections are also extensively studied in terms of time-varying loads. In [13], a bolt connection of a steel beam with a column with an end-plate subjected to cyclic loading is analyzed. In [14], a three-dimensional macromodel of the connection under cyclic loading conditions is presented. A nonlinear time-history analysis of three-dimensional frames is presented in [15], in which geometrical nonlinearity is taken into account.

An extended nonlinear dynamic analysis of slender frames with semi-rigid connections is explored in [16], where equilibrium paths are obtained by continuation techniques and using the Newton–Raphson method. The results of both theoretical and experimental research on the dynamics of portal steel frames can be found in [17–22]. In [23] experimental tests were presented, which aimed to determine the response of the structure to seismic loads.

BAYAT and ZAHRAI [24] present an analysis of steel frames with rigid and semi-rigid connections. Five earthquake records were selected as the load. In [25] a model of rotational cyclic behavior of the base plate was presented using the component method.

In [26], a model of the connection in ABAQUS program was created, which was subjected to cyclic loads. The geometrical and material nonlinearities were taken into account. Geometrical nonlinearities in the analysis of three-dimensional semi-rigid frames subjected to dynamic loads are presented in [27]. Extensive overview of structures with semi-rigid connections can be found in [28].

OZEL *et al.* [29] present a method of estimating dynamic characteristics in a steel frame, which takes into account the presence of semi-rigid connections and the influence of accurate modeling of shear deformations. The study provides solutions obtained in the ANSYS program.

The use of a viscoelastic material in the connection may have a beneficial effect on the reduction of vibrations in structures loaded with dynamic forces [30]. There are various ways of incorporating viscoelastic material into a node. In reinforced concrete structures, polymeric materials are used as pads in supports. In this work, the studies are devoted to connections where the viscoelastic material affects the rotation of the cross-section at the node, where the hinge transfers axial and shear forces, and the viscoelastic material constrains the rotation. Connections of this type occur in steel structures, examples of such nodes are studied in [31] and [32].

The equation of motion describing the dynamic behavior of a viscoelastic material can be related to a mechanical model built of properly connected dashpots and springs. In the literature, there are classical models (e.g. the Kelvin or Maxwell model) and the so-called fractional models, including an element described by non-integer derivatives, which has both viscous and elastic properties (e.g. the Scott–Blair element). The use of fractional derivatives instead of integer derivatives to model the rheological properties of viscoelastic materials has been presented in [33, 34]. Fractional models are popular because, with a small number of parameters, they can accurately describe the dynamic behaviour of the viscoelastic material for different temperatures and different frequencies. The analysis of steel frames with semi-rigid viscoelastic connections, both in the frequency and time domain, is presented in [35]. Parametric studies of response spectra for recorded and artificial earth motions for viscoelastic bonds described by the Generalized Maxwell model and the equivalent Kelvin–Voigt model were carried out. Complex modal analyzes aimed at determining the dynamic characteristics of the frame and examining the effect of the stiffness of the connection and the rotary damper on natural frequencies and modal damping coefficients are also presented in [31, 36].

Papers in which theoretical research is confirmed by experimental results are rather rare. In the work [37], the natural frequencies of the L-type steel frame and the portal frame with rotational springs symbolizing semi-rigid connections were numerically analyzed and compared with the experimental results. The dynamic characteristics of structures with viscoelastic elements are determined in [38], where the equations of motion are presented in the frequency domain, and then a properly defined eigenproblem is solved using the continuation method. The continuation method is used to solve a nonlinear eigenproblem in systems with viscoelastic elements [38–41], as well as to solve nonlinear equations of amplitudes [42].

This article presents the derivation of the stiffness matrix, the consistent mass matrix and the damping matrix for a beam element with rotational viscoelastic constraints. The Euler Bernoulli beam model under small displacements was adopted for the analyses. The linearly elastic material was adopted along the length of the element and in semi-rigid connections. The modified finite element and derived matrices were used for the modal analysis of frame structures using the ordinary FEM method. Shear deformations have not been considered in the beam element. Taking them into account in the energy balance is possible and would lead to the development of appropriate matrices for the Timoshenko beam. Such a problem was discussed in [43], where shear deformations were also taken into account in order to determine the damping of the system.

An alternative way of taking into account the viscoelastic connections in frame structures is also presented in the article. It consists of treating the viscoelastic element as an additional constraint connecting the appropriate degrees of freedom. In this approach, a fractional rheological model was used to describe the viscoelastic bond, which resulted in the nonlinear eigenproblem. In order to solve the eigenproblem, the continuation method was chosen, the procedure of which is also briefly described. Finally, several computational examples demonstrating the effectiveness of the proposed method are presented, and the paper is summarized with concluding remarks.

2. Finite element with viscoelastic bonds

In the first approach to the static and dynamic analysis of a frame structure with viscoelastic nodes, the classical finite element method (FEM) was used, which required the determination of an appropriate finite element. For this purpose, stiffness, mass and damping matrices were derived for a finite element containing viscoelastic constraints. Moreover, in the following considerations, it was assumed that elastic constraints and viscous constraints occur in both nodes of a finite element, but only in relation to the rotational degrees of freedom.

2.1. Stiffness matrix

In a six-degree-of-freedom beam finite element that has length L and bending stiffness EI , the values of the rotational stiffness at the support nodes are defined as k_0 and k_l , respectively. Moreover, it was assumed that the damping coefficients, denoted as c_0 and c_l , are defined in relation to the rotational constraints in the nodes. The connection of the beam element with supports by means of rotational elastic and viscous constraints is shown symbolically in Fig. 1. It has been assumed that the sections denoted as e_0 and e_l are infinitely stiff and infinitely short, so the lengths L and l are equal.

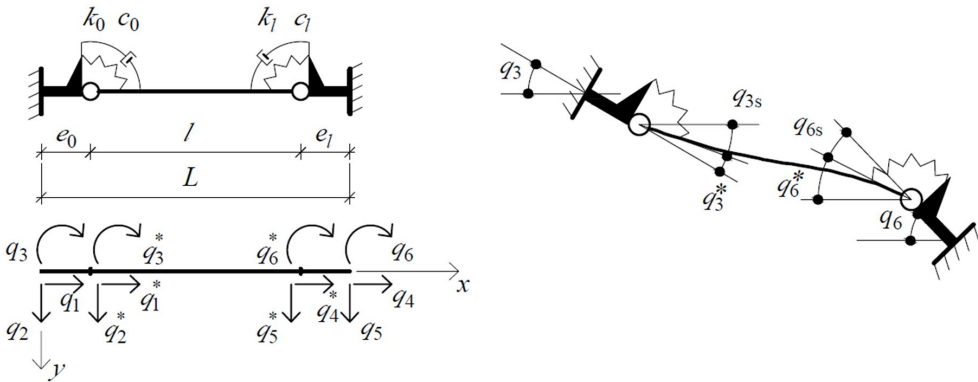


FIG. 1. Beam finite element with viscoelastic rotational bonds.

Figure 1 shows nodal displacements of the beam element (marked with asterisks) and displacements in the supports. The nodal translational displacements of the beam element are the same as the displacements of the supports, i.e.:

$$q_1 = q_1^*, \quad q_2 = q_2^*, \quad q_4 = q_4^*, \quad q_5 = q_5^*,$$

while the rotations of the supports differ from the nodal rotations of the beam due to the rotational flexibility of the connections:

$$(2.1) \quad q_3 = q_3^* + q_{3s}, \quad q_6 = q_6^* + q_{6s}.$$

Rotation angles in elastic constraints can be determined by the relationships:

$$(2.2) \quad q_{3s} = \frac{Q_3^*}{k_0}, \quad q_{6s} = \frac{Q_6^*}{k_l}.$$

Using Eqs. (2.1) and (2.2), the stiffness matrix of a beam element with rotational flexibility can be determined in the following form:

$$(2.3) \quad \tilde{\mathbf{K}} = \begin{bmatrix} k_1 & 0 & 0 & -k_1 & 0 & 0 \\ 0 & k_{11} & k_{12} & 0 & k_{13} & k_{14} \\ 0 & k_{21} & k_{22} & 0 & k_{23} & k_{24} \\ -k_1 & 0 & 0 & k_1 & 0 & 0 \\ 0 & k_{31} & k_{32} & 0 & k_{33} & k_{34} \\ 0 & k_{41} & k_{42} & 0 & k_{43} & k_{44} \end{bmatrix},$$

where:

$$(2.4) \quad \begin{aligned} k_{11} &= \frac{12EI}{l^3\Omega}(1 + \mu_0 + \mu_l), & k_{12} &= k_{21} = \frac{6EI}{l^2\Omega}(1 + 2\mu_l), \\ k_{14} &= k_{41} = \frac{6EI}{l^2\Omega}(1 + 2\mu_0), & k_{22} &= \frac{4EI}{l\Omega}(1 + 3\mu_l), \\ k_{23} &= k_{32} = -\frac{6EI}{l^2\Omega}(1 + 2\mu_l), & k_{24} &= k_{42} = \frac{2EI}{l\Omega}, \\ k_{33} &= \frac{12EI}{l^3\Omega}(1 + \mu_0 + \mu_l), & k_{13} &= k_{31} = -\frac{12EI}{l^2\Omega}(1 + \mu_0 + \mu_l), \\ k_{34} &= k_{43} = -\frac{6EI}{l^2\Omega}(1 + 2\mu_0), & k_{44} &= \frac{4EI}{l\Omega}(1 + 3\mu_0), \\ \mu_0 &= \frac{EI}{k_0l}, & \mu_l &= \frac{EI}{k_l l}, \\ k_1 &= \frac{EA}{l}, & \Omega &= (1 + 4\mu_0 + 4\mu_l + 12\mu_0\mu_l). \end{aligned}$$

2.2. Mass matrix

Assuming a constant mass density ρ along the element, a consistent mass matrix $\tilde{\mathbf{M}}_e$ for a finite element with given viscoelastic rotational bonds at nodes can be presented as a sum of two matrices [37]:

$$(2.5) \quad \tilde{\mathbf{M}}_e = \tilde{\mathbf{M}}_k + \tilde{\mathbf{M}}_m.$$

The basic $\tilde{\mathbf{M}}_k$ matrix that contains classical components related to elastic constraints:

$$(2.6) \quad \tilde{\mathbf{M}}_k = \frac{\rho l}{420} \begin{bmatrix} 140 & & & & & \\ 0 & 4Z_1(v_1, v_2) & & & & \text{Symmetry} \\ 0 & 2lZ_2(v_1, v_2) & 4l^2Z_5(v_1, v_2) & & & \\ 70 & 0 & 0 & 140 & & \\ 0 & 2Z_3(v_1, v_2) & lZ_4(v_2, v_1) & 0 & 4Z_1(v_2, v_1) & \\ 0 & -lZ_4(v_1, v_2) & -l^2Z_6(v_1, v_2) & 0 & -2lZ_2(v_2, v_1) & 4l^2Z_5(v_2, v_1) \end{bmatrix}$$

the displacement vector, $\mathbf{p}(t)$ is the excitation force vector, and $\mathbf{f}(t)$ is the vector of forces generated in viscoelastic bonds, which are treated as an additional load. Graphically, additional constraints are represented as viscoelastic rotary connectors (VRC) that are associated with the appropriate degrees of freedom of the structure. The method of introducing rotational bonds in an exemplary node of a frame structure is shown in Fig. 2. The vector of additional forces for the entire structure is the sum of vectors $\mathbf{f}_r(t)$, i.e. vectors of forces caused by the VRC elements:

$$(3.2) \quad \mathbf{f}(t) = \sum_{r=1}^m \mathbf{f}_r(t),$$

where m is the total number of VRCs.

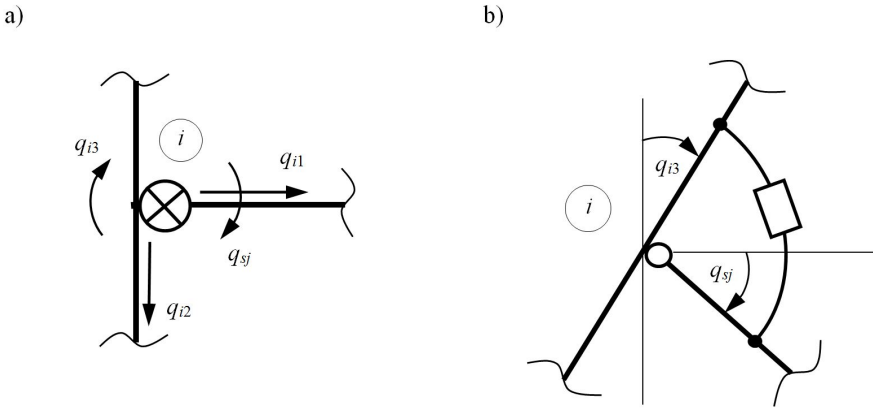


FIG. 2. Viscoelastic connection treated as an additional constraint between rotational degrees of freedom.

Applying the Laplace transformation with zero initial conditions, the equation of motion (3.1) could be written as follows:

$$(3.3) \quad (s^2\mathbf{M} + s\mathbf{C} + \mathbf{K})\bar{\mathbf{q}}(s) = \bar{\mathbf{p}}(s) + \bar{\mathbf{f}}(s),$$

where

$$(3.4) \quad \bar{\mathbf{f}}(s) = \sum_{r=1}^m \bar{\mathbf{f}}_r(s)$$

and s is the Laplace variable, $\bar{\mathbf{q}}(s)$ is the Laplace transform of $\mathbf{q}(t)$ and $\bar{\mathbf{p}}(s)$ is the Laplace transform of $\mathbf{p}(t)$.

If only one VRC element (e.g. number r) is mounted on the structure in such a way that the ends of the element coincide with the i -th and j -th degree of

freedom of the structure, respectively (Fig. 3b), then the Laplace transform of the forces vector can be written in the following form:

$$(3.5) \quad \bar{\mathbf{f}}_r(s) = -(K_r + G_r(s))\mathbf{L}_r\bar{\mathbf{q}}(s),$$

where \mathbf{L}_r is the $(n \times n)$ global location matrix of the element. The location matrix for the selected VRC element is built using the allocation vector \mathbf{e}_r (r -th element). If the element r is mounted on a structure between degrees of freedom number i and j , then the location matrix is given by $\mathbf{L}_r = \mathbf{e}_r\mathbf{e}_r^T$, where $\mathbf{e}_r = \text{col}(0, \dots, e_i = 1, \dots, e_j = -1, \dots, 0)$.

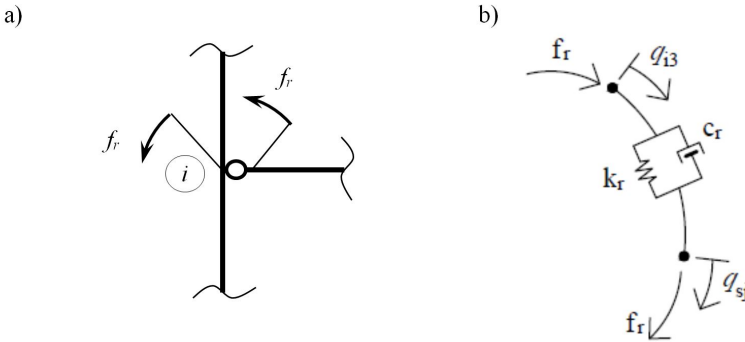


FIG. 3. Additional forces acting in the structure node and in the viscoelastic rotary connector (VRC).

The total vector of the Laplace transforms of the interaction forces that act between the VRC elements and the structure can be written as:

$$(3.6) \quad \bar{\mathbf{f}}(s) = -\sum_{r=1}^m (K_r + G_r(s))\mathbf{L}_r\bar{\mathbf{q}}(s).$$

The final form of the equation of motion for the structure with VRCs, written in the frequency domain, is:

$$(3.7) \quad (s^2\mathbf{M} + s\mathbf{C} + \mathbf{G}_d(s) + \mathbf{K} + \mathbf{K}_d)\bar{\mathbf{q}}(s) = \mathbf{0},$$

where $\mathbf{K}_d = \sum_{r=1}^m K_r\mathbf{L}_r$, $\mathbf{G}_d(s) = \sum_{r=1}^m G_r(s)\mathbf{L}_r$ and $\bar{\mathbf{p}}(s) = \mathbf{0}$, K_r and $G_r(s)$ are functions describing the elastic and viscous properties of the adopted rheological model of the connection. Equation (3.7) constitutes the nonlinear eigenvalue problem. Dynamic characteristics of the structure, such as natural frequencies ω_i and non-dimensional damping ratios γ_i can be determined on the basis of obtained eigenvalues s_i :

$$(3.8) \quad \omega_i^2 = \mu_i^2 + \eta_i^2, \quad \gamma_i = -\mu_i/\omega_i,$$

where $\mu_i = \text{Re}(s_i)$, $\eta_i = \text{Im}(s_i)$.

In the case of classical rheological models, it is possible to linearize the eigenproblem, whereas in the case of fractional models, one of the methods of solving the nonlinear eigenproblem should be used, e.g. the continuation method.

3.1. Classical rheological model of rotational constraints

The force generated by the viscoelastic rotational constraint (Fig. 3) can be expressed as the sum of the elastic force and the damping force:

$$(3.9) \quad f_r(t) = k_r \Delta q(t) + c_r \Delta \dot{q}(t),$$

where:

$$\Delta q(t) = q_j - q_i, \quad \dot{q}_k(t) = \frac{d}{dt} q_k.$$

Equation (3.9) describes the rheological model, known as the classical Kelvin model with the given parameters of elasticity k_r and viscosity c_r . In this case, the functions in formula (3.6) are: $K_r = k_r$ and $G_r(s) = s c_r$.

3.2. Fractional rheological model of rotational constraints

If the element related to viscosity in the Kelvin model (Fig. 3) is replaced by a viscoelastic element, i.e. the so-called Scott–Blair element, the fractional rheological model will be obtained. The Scott–Blair element, whose graphic symbol is a rhombus (Fig. 4), is described by two parameters: the constant c_r and the number α , which is a non-integer number ($0 < \alpha \leq 1$) that determines the order of the derivative with respect to time.

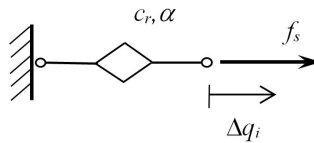


FIG. 4. The Scott–Blair element symbolizing the fractional rheological model.

The constitutive equation for the above-mentioned Scott–Blair element can be written in the following form:

$$(3.10) \quad f_s(t) = c_r D_t^\alpha \Delta q(t)$$

where the symbol $D_t^\alpha(\cdot)$ denotes the fractional-derivative of the order α with respect to the time t . In this work we adopt the Riemann–Liouville definition of fractional derivatives [33, 34].

If the fractional Kelvin model is used to describe a viscoelastic connection, the functions in formula (3.6) are: $K_r = k_r$ and $G_r(s) = s^\alpha c_r$.

4. Nonlinear eigenproblem – the continuation method

The continuation method described in [38] and briefly presented in this Section was used to solve the nonlinear eigenproblem. According to this method, the parameter κ is introduced into the equation to be solved, i.e. the equation of motion (3.7). After neglecting the internal damping of the structure ($\mathbf{C} = \mathbf{0}$), Eq. (3.7) can be rewritten as follows:

$$(4.1) \quad \mathbf{h}_1(s, \mathbf{q}) = \mathbf{D}(s)\mathbf{q}(s) = \mathbf{0},$$

where

$$\mathbf{D}(s) = s^2\mathbf{M} + \kappa\mathbf{G}_d(s) + \mathbf{K} + \mathbf{K}_d.$$

Equation (4.1) has $n + 1$ unknowns, therefore it is necessary to add one more equation. Following the work [33], it was proposed that the additional equation was a way to normalize the eigenvector \mathbf{q} :

$$(4.2) \quad h_2(s, \mathbf{q}) = \mathbf{q}^T(s) \frac{\partial \mathbf{D}(s)}{\partial s} \mathbf{q}(s) - a = 0,$$

where a is a given value (see Eq. (4.6)) and

$$(4.3) \quad \frac{\partial \mathbf{D}(s)}{\partial s} = 2s\mathbf{M} + \kappa \frac{\partial \mathbf{G}_d(s)}{\partial s}.$$

Parameter κ increases incrementally from 0 to 1, and for the increment l it can be written as

$$(4.4) \quad \kappa_l = \kappa_{l-1} + \Delta\kappa,$$

where $\Delta\kappa$ is the assumed increment, e.g. $\Delta\kappa = 0.1$.

The initial step of iteration is determined after substituting $\kappa = 0$, which transforms the nonlinear eigenproblem (4.1) into a linear eigenproblem:

$$(4.5) \quad (s_0^2\mathbf{M} + \mathbf{K} + \mathbf{K}_d)\mathbf{q}_0(s) = \mathbf{0}.$$

The solutions of Eq. (4.5) are the real eigenvalues s_0 and the corresponding real eigenvectors \mathbf{q}_0 . The constant a can be calculated as:

$$(4.6) \quad a = s_0\mathbf{q}_0^T\mathbf{M}\mathbf{q}_0.$$

The values s_0 and \mathbf{q}_0 are taken as the starting point of the iterations to find complex eigenvalues and eigenvectors, which are the solutions of the eigenproblem (4.1). Then, in each increment of κ , successive approximations of the solution are carried out by determining the increments of eigenvalues and eigenvectors

using the Newton method. For the iteration step t , the incremental equations of the Newton method written based on the system of Eqs. (4.1) and (4.2) are as follows:

$$(4.7) \quad \begin{aligned} \frac{\partial \mathbf{h}_1}{\partial \mathbf{q}} \bigg|_{\substack{s=s_l^{(t)} \\ \mathbf{q}=\mathbf{q}_l^{(t)}}} \delta \mathbf{q} + \frac{\partial \mathbf{h}_1}{\partial s} \bigg|_{\substack{s=s_l^{(t)} \\ \mathbf{q}=\mathbf{q}_l^{(t)}}} \delta s &= -\mathbf{h}_1(s_l^{(t)}, \mathbf{q}_l^{(t)}), \\ \frac{\partial h_2}{\partial \mathbf{q}} \bigg|_{\substack{s=s_l^{(t)} \\ \mathbf{q}=\mathbf{q}_l^{(t)}}} \delta \mathbf{q} + \frac{\partial h_2}{\partial s} \bigg|_{\substack{s=s_l^{(t)} \\ \mathbf{q}=\mathbf{q}_l^{(t)}}} \delta s &= -h_2(s_l^{(t)}, \mathbf{q}_l^{(t)}), \end{aligned}$$

where:

$$\begin{aligned} \frac{\partial \mathbf{h}_1}{\partial \mathbf{q}} &= s^2 \mathbf{M} + \kappa_l \mathbf{G}_d(s) + \mathbf{K} + \mathbf{K}_d, \\ \frac{\partial \mathbf{h}_1}{\partial s} &= \left(2s \mathbf{M} + \kappa_l \frac{\partial \mathbf{G}_d(s)}{\partial s} \right) \mathbf{q}, \\ \frac{\partial h_2}{\partial \mathbf{q}} &= \mathbf{q}^T \left(2s \mathbf{M} + \kappa_l \frac{\partial \mathbf{G}_d(s)}{\partial s} \right), \\ \frac{\partial h_2}{\partial s} &= \mathbf{q}^T \left(2 \mathbf{M} + \kappa_l \frac{\partial^2 \mathbf{G}_d(s)}{\partial s^2} \right) \mathbf{q}. \end{aligned}$$

The new approximation of eigenvalues and eigenvectors for the iterative step t is calculated as:

$$(4.8) \quad \begin{aligned} s_l^{(t)} &= s_l^{(t-1)} + \delta s, \\ \mathbf{q}_l^{(t)} &= \mathbf{q}_l^{(t-1)} + \delta \mathbf{q}. \end{aligned}$$

The iterative process is completed when the following conditions are satisfied:

$$(4.9) \quad \begin{aligned} |s_l^{(t)} - s_l^{(t-1)}| &\leq \varepsilon_1 |s_l^{(t)}|, \\ \|\mathbf{q}_l^t - \mathbf{q}_l^{t-1}\| &\leq \varepsilon_2 \|\mathbf{q}_l^t\|, \end{aligned}$$

where ε_1 and ε_2 are sufficiently small numbers, the assumed accuracies of calculations.

The final solution is obtained for $\kappa = 1$. The above-described procedure of the continuation method should be applied sequentially for each searched eigenvalue.

The flowchart of the continuation method is shown in Fig. 5.

5. Numerical examples

In order to validate the proposed procedures, numerical calculations were performed for a few selected structures. The solutions obtained using a modified

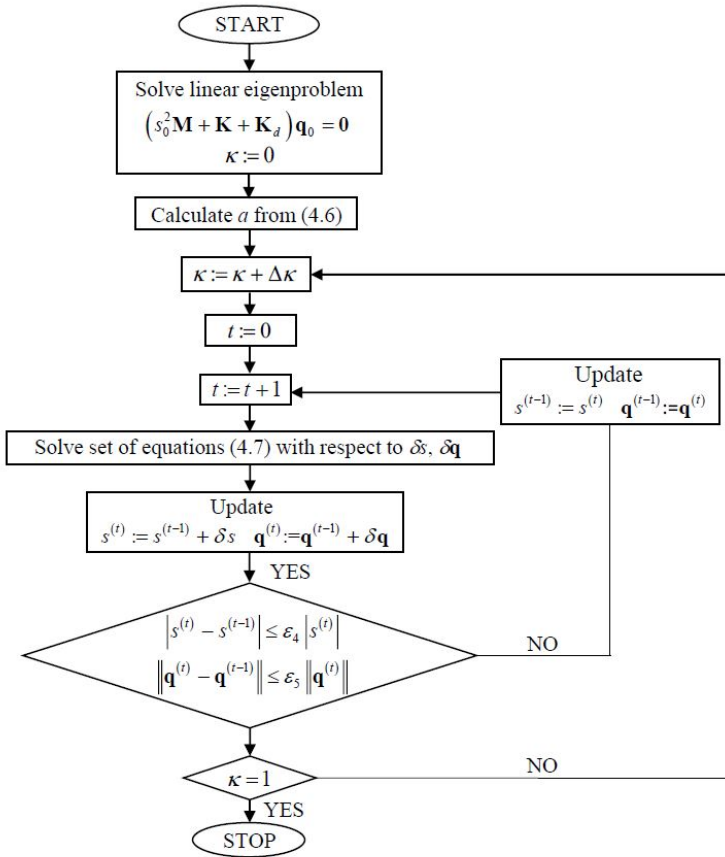


FIG. 5. The flowchart of the continuation method.

finite element with viscoelastic bonds were compared with the solutions obtained for structures in which the viscoelastic joints were treated as additional bonds between the elements.

5.1. Beam with viscoelastic bonds at the supports

A single-span beam made of I-section IPE 300 was analyzed (Fig. 6). Young’s modulus $E = 205$ GPa and beam spans $L = 10$ m were assumed. The considered structure was supported at both ends by hinges and additionally by rotational viscoelastic bonds. The proposed approach makes it possible to investigate the influence of the rotational flexibility of the supports on the dynamic response of the structure. The values of the rotational flexibility coefficients were determined in relation to the bending stiffness of the beam, i.e. $k_i = \alpha_1 EI$, where α_1 is the coefficient varying in a certain range, and I is the cross-section moment of inertia.

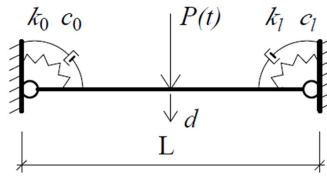


FIG. 6. Beam with rotational viscoelastic bonds.

Figure 6 shows the diagrams of changes in the first natural frequency ω_1 of the considered beam, as a functions of the rotational flexibility coefficients k_0 and k_l .

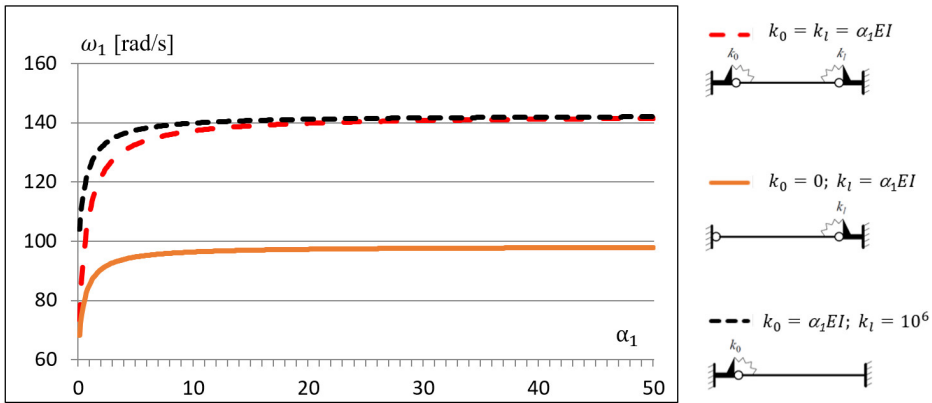


FIG. 7. The first natural frequency ω_1 versus the rotational flexibility coefficients.

When the rotational flexibility coefficient approaches zero, the support may be treated as a hinge, and when the value of this coefficient is several orders greater than the beam bending stiffness, the support is treated as a fixed. Based on the results presented in Fig. 7, it can be concluded that the dynamic parameters of the structure are almost constant when the rotational flexibility coefficient exceeds the bending stiffness of the beam several times.

In the next test, the dynamic response of the structure was determined. The amplitude of the vertical displacement d (Fig. 6) caused by the vertical dynamic force $P(t) = P_0 \cos \lambda t$, where $P_0 = 1.0 \text{ MN}$ was calculated for the increasing excitation frequency λ . Figure 8 presents the results, i.e. resonance curves for selected values of damping coefficients c_0 and c_l . The values of the rotational damping coefficients were adopted in relation to the bending stiffness of the analyzed beam, i.e. $c_i = \alpha_2 EI$, where α_2 takes one of the selected values: 0, 0.001, 0.005 or 0.01 [s · Nm/rad]. On the other hand, the values of the stiffness coefficients were the same in all dynamic tests, i.e. $k_0 = k_l = 0.2 EI$.

In Fig. 8, the green dashed line shows solutions for $\alpha_2 = 0$, which correspond to the case when there is no damping in the system ($c_i = 0$). In this case, the displacement amplitudes at resonance frequencies tend to infinity (vertical asymptotes).

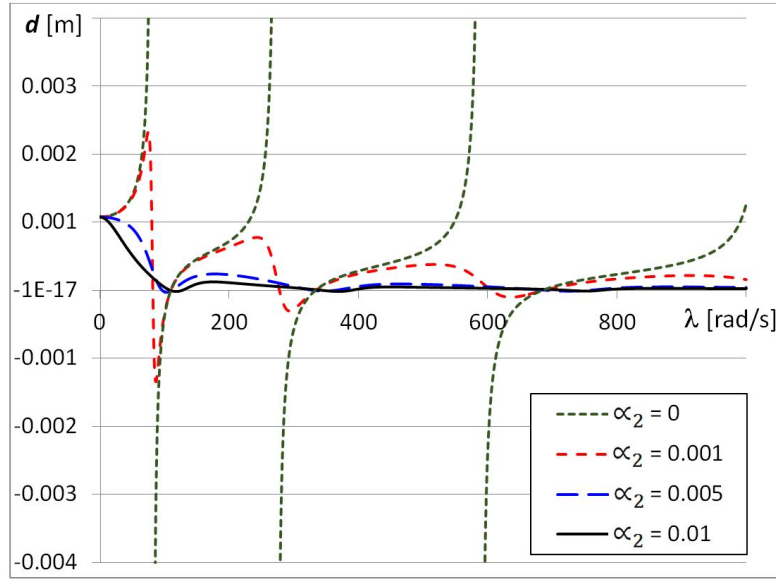


FIG. 8. The resonance curves for different values of the damping coefficient c_0 and c_i .

The successive curves refer to the solutions for the next selected values of damping coefficients ($c_i = \alpha_2 EI$). The black solid line shows the solution for the highest assumed value of the damping coefficients c_i . As a result of dynamic analysis, it can be concluded that the increasing value of the damping coefficient does not change the resonant frequency, but significantly reduces the dynamic response of the structure.

5.2. L-type frame with semi-rigid connection

In this example, a structure composed of two elements is analyzed, the so-called L-type frame with a semi-rigid internal joint (Fig. 9). Data describing the structure and some results of dynamic analyzes were taken from [44]. The following data were adopted for the calculations: Young's modulus $E = 200$ GPa, bending stiffness $EI = 41.48$ Nm², mass distribution $\rho = 11.08$ Ns²/m² and rotational flexibility $k = 137.3$ Nm/rad [44].

Table 1 shows the results of the modal analysis, the natural frequency values obtained assuming a rigid connection in the middle node and those obtained assuming that this connection is flexible.

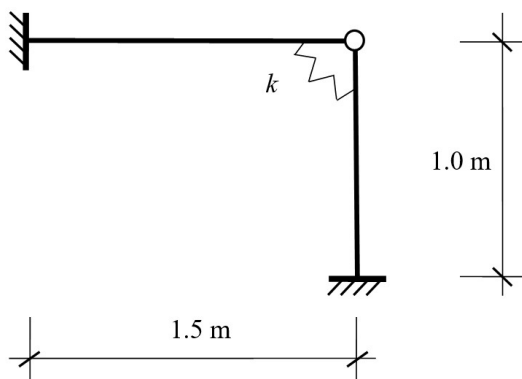


FIG. 9. L-type frame model with semi-rigid connection.

TABLE 1. Natural frequency values for different types of internal connection.

Types of connection	Mode	SILVA <i>et. al.</i> [44] ω_i [rad/s]	Present work ω_i [rad/s]
Rigid	1	15.81	15.82
	2	34.74	34.85
Flexible	1	14.90	14.91
	2	32.72	32.87

Table 2 lists the natural frequencies ω [rad/s] obtained with various discretizations of the structure, both for the rigid connection and for the flexible connection in the internal node. In each case both the column and the beam were divided into the same number of finite elements.

TABLE 2. Natural frequencies ω_i [rad/s] for different discretizations, for rigid and for flexible connection.

Type of connection	Mode	Number of finite elements in a member				
		1 element	2 elements	4 elements	10 elements	100 elements
Rigid	1	24.47	16.01	15.84	15.82	15.82
	2	4519.15	35.62	34.91	34.86	34.85
Flexible	1	32.52	15.13	14.92	14.91	14.91
	2	4698.38	33.32	32.90	32.87	32.87

The results from Table 2 can be summarized that the proposed approach leads to accurate results with relatively coarse discretization, even when dividing a structural member into four finite elements.

5.3. L-type frame with viscoelastic connection

In the second example concerning the L-type frame (Fig. 10), the connection in the inner node was described by the rotational stiffness coefficient $k = 120 \text{ Nm/rad}$, and also by the damping coefficient $c = 0.25 \text{ Nm}\cdot\text{s/rad}$. A structure made of a beam and a column with the same bending stiffness $EI = 75.7 \text{ Nm}^2$ and mass distribution $\rho = 72.01 \text{ kg/m}$ was adopted for the analysis.

First, dynamic analyzes were performed, assuming that only rotational elasticity k was set in the internal node ($c = 0$). This made it possible to compare the obtained results with the results reported in [37]. Table 3 lists four natural frequencies determined by different methods for the frame with a rigid connection and for the frame with a semi-rigid connection. It is worth noting, that the results given in [37] were obtained by computational methods as well as experimentally.

TABLE 3. Natural frequencies ω_i [rad/s] determined by various methods, including experimental ones.

Mode	Rigid connection		Semi rigid connection		
	KAWASHIMA <i>et al.</i> [37] Calculated	Present method	KAWASHIMA <i>et al.</i> [37] Calculated	KAWASHIMA <i>et al.</i> [37] Experimental	Present method
1	23.3	23.32	21.6	21.0	20.84
2	51.4	51.36	47.8	46.0	46.26
3	74.5	73.97	67.2	65.0	65.05
4	142.8	135.55	142.9	138.0	134.15

In the next analysis, the dynamic response of the structure, the so-called resonance curves, were determined for selected values of the damping coefficient c . Figure 10 shows the calculation results, i.e. the amplitude of the cross-section rotation at the load point (point B in Fig. 10) caused by the dynamic moment $M(t) = M_0 \cos \lambda t$, where $M_0 = 1.0 \text{ MNm}$, for the increasing value of the excitation frequency λ .

In Fig. 11, the red dashed line shows the solutions obtained when the damping in the internal node was neglected ($c = 0$). In this case, the displacement amplitudes at resonant frequencies tend to infinity, also for the first natural frequency $\omega_i = 20.84 \text{ rad/s}$.

The solid black line shows solutions for the highest assumed damping value $c = 0.033 EI = 2.5 \text{ Nm s/rad}$. In all the cases, the elasticity of the joint was the same $k = 1.585 EI = 120 \text{ Nm/rad}$.

The effectiveness of damping occurring in the internal node is particularly noticeable in the resonance zones. The relatively small value of the damping

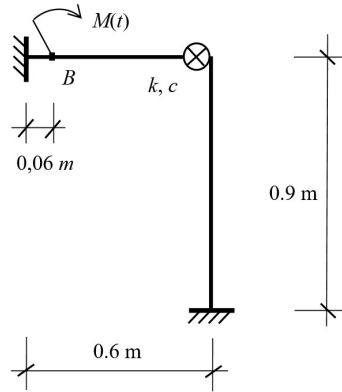


FIG. 10. L-type frame structure with a rotational viscoelastic connection.

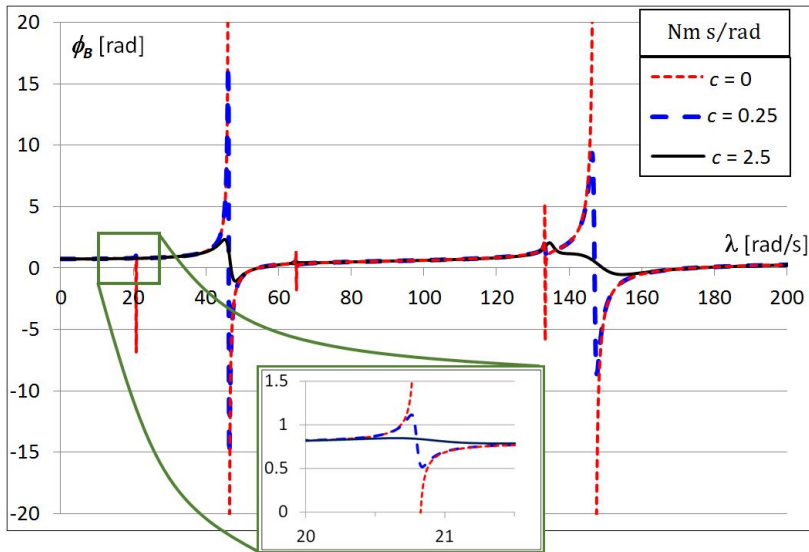


FIG. 11. Resonance curves (rotation of the cross-section at point B) for selected damping coefficients c .

coefficient c significantly reduces the dynamic response of the structure, even when the retardation time is very short: $c/k = 0.0208$ s.

5.4. Portal frame with internal viscoelastic nodes

A portal frame made of HEA 300 steel profile was also analyzed. Rotational viscoelastic bonds were assumed in the corners of the frame, in the beam-to-column connections (Fig. 12).

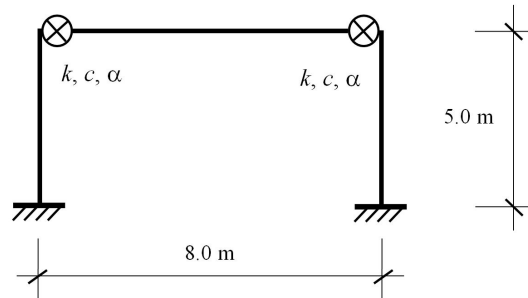


FIG. 12. Model of a portal frame with two viscoelastic internal nodes.

The fractional Kelvin model defined by the parameters c , k and α was adopted for the rheological description of rotational viscoelastic bonds. In the first stage of the calculations, the fundamental natural frequencies of the frame with rigid nodes were compared with the solutions for the frame with flexible nodes. Table 4 compares six natural frequencies determined by two different methods described in previous chapters, i.e. using a modified finite element and by introducing additional viscoelastic bonds in the structure. For a semi-rigid connection, the stiffness coefficient $k = 0.2 EI = 7\,669 \text{ kNm/rad}$ was assumed.

TABLE 4. Natural vibrations frequencies ω_i [rad/s] determined by different methods.

Mode	Rigid connection		Semi rigid connection	
	Modified finite element	Addition of viscoelastic bonds	Modified finite element	Addition of viscoelastic bonds
1	67.800	67.798	54.120	54.120
2	159.34	159.34	121.86	121.86
3	413.96	413.96	410.75	410.75
4	488.55	488.53	422.96	422.96
5	622.15	622.11	469.77	469.77
6	975.17	975.15	898.25	898.20

The results in Table 4 obtained by both methods mentioned above are almost identical. In this case, the relative differences in values do not exceed one hundredth of a percent.

In the subsequent analyses, the influence of the damping coefficients c on the solution was investigated. Modal characteristics of the structure (ω_i, γ_i) were determined for selected values of coefficients c and α . Table 5 and Fig. 13 show the

change of the natural frequency for the increasing value of the damping coefficient c . The value of c was determined in relation to the rotational elasticity k , which was constant for all the analyzed cases, i.e. $k = 0.2 EI$.

TABLE 5. Natural vibrations frequencies ω_i [rad/s] for the increasing value of the damping coefficient c .

Mode	$c = 0.0$	$c = 0.001 k$	$c = 0.003 k$	$c = 0.006 k$	$c = 0.01 k$
1	54.120	54.125	54.172	54.328	54.697
2	121.856	121.915	122.395	124.032	127.971
3	410.752	411.100	412.495	413.432	413.754
4	422.961	423.567	428.328	442.477	462.163
5	469.771	470.997	482.780	526.758	580.189

Figure 13 shows the obtained results, i.e. the change in natural frequency: $\tilde{\omega}_i$ determined using a modified finite element (lines on the diagram) and ω_i obtained by the second method, i.e. by introducing additional viscoelastic bonds into the structure (point markers on the diagram).

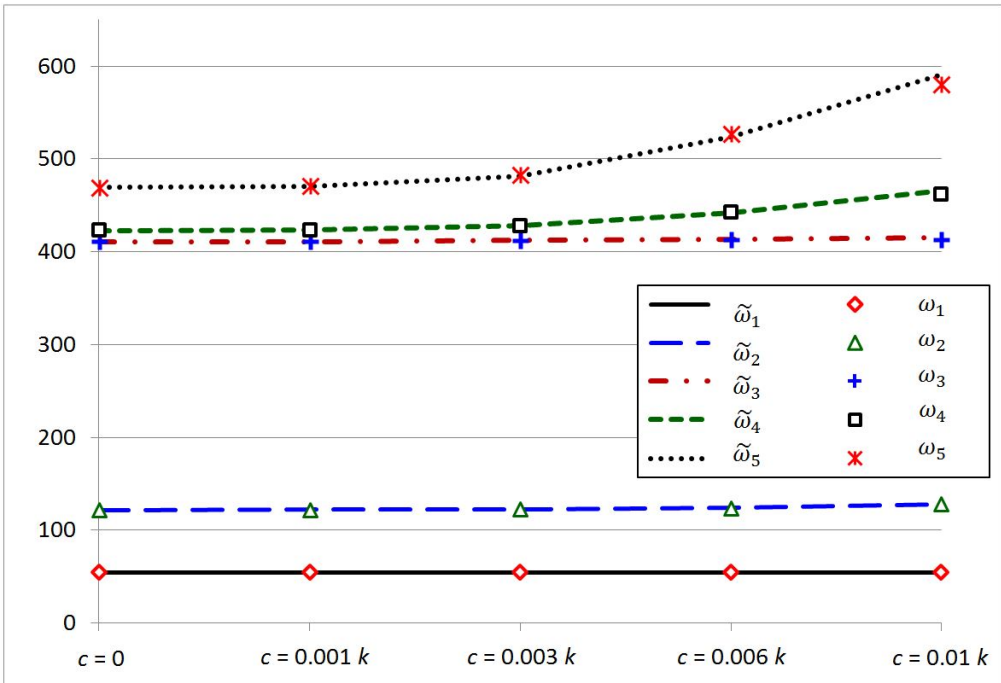


FIG. 13. Natural vibrations frequencies ω_i and $\tilde{\omega}_i$ [rad/s] for the increasing value of the damping coefficient c .

The increasing value of the damping coefficient in the considered example causes significant changes only for higher natural frequencies of the structure (Fig. 13).

In the following analyses, rotational constraints at the corners of the frame are described by a fractional Kelvin model, which is determined by three parameters: k , c and α . Such an analysis is only possible using the second method, where viscoelasticity is introduced into the structure as additional rotational bonds at the nodes. In the analysis, it was assumed that the parameters k and c were constant ($k = 0.2 EI$, $c = 0.01 k$), and only the parameter α varied from 0.6 to 1.0. It is worth noting that when the parameter α reaches one ($\alpha = 1$), the fractional Kelvin model turns into the classical Kelvin model. The obtained values of the natural frequencies ω_i presented in Table 6 show little sensitivity to the change of the parameter α in the considered range. However, the change in the value of the non-dimensional damping ratio γ_i is significant (Table 7). It can be concluded that in the considered frame the non-dimensional damping ratio of the second mode is the parameter most sensitive to the variation of the parameter α (Fig. 14).

TABLE 6. Natural vibrations frequencies ω_i [rad/s] for the increasing value of the parameter α .

Mode	$\alpha = 0.6$	$\alpha = 0.7$	$\alpha = 0.8$	$\alpha = 0.9$	$\alpha = 1.0$
1	54.4841	54.5620	54.6306	54.6775	54.6970
2	123.3001	123.8072	124.4776	125.5462	127.9714
3	411.3816	411.7963	412.4599	413.2281	413.7543
4	426.6232	428.7702	432.7380	441.7993	462.1632

TABLE 7. Non-dimensional damping ratios γ_i [-] for the increasing value of the parameter α .

Mode	$\alpha = 0.6$	$\alpha = 0.7$	$\alpha = 0.8$	$\alpha = 0.9$	$\alpha = 1.0$
1	0.0086	0.0140	0.0222	0.0346	0.0537
2	0.0147	0.0256	0.0435	0.0726	0.1204
3	0.0014	0.0022	0.0029	0.0028	0.0020
4	0.0103	0.0198	0.0361	0.0602	0.0776

In general, increasing the α parameter leads to an improvement in the damping properties in the viscoelastic nodes and an improvement in the damping properties of the entire structure.

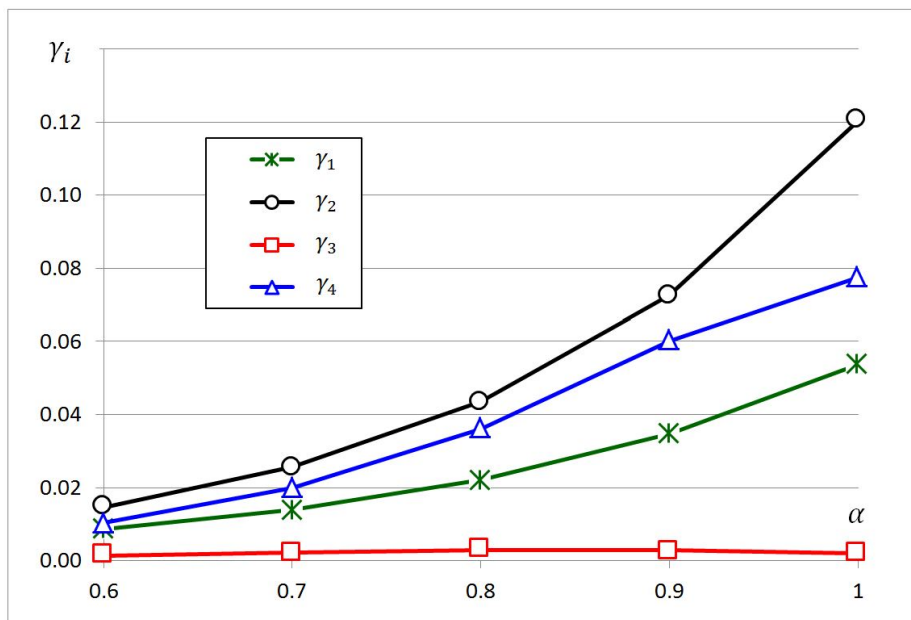


FIG. 14. Non-dimensional damping ratios γ_i [-] versus the value of the parameter α .

6. Conclusions

The subject of the research was the dynamic analysis of frame structures in which viscoelastic connections in the form of rotational bonds occur in the nodes. In addition to the traditional finite element approach, which required the development of an appropriate finite element, a second approach was proposed, in which additional rotational constraints were introduced into the system. The development of a finite element that takes into account viscoelastic bonds, even for a simple rheological model for these bonds, leads to complex formulas for the coefficients of mass and stiffness matrices. On the other hand, the second approach, which consists in adding viscoelastic bonds in a frame structure, allows an easy application of any rheological model for these bonds. In this work, the fractional Kelvin model was used to describe rotational viscoelastic bonds, which is characterized by only three parameters, but its constitutive equation contains fractional order derivatives. The use of fractional derivatives to describe the damping properties led to a non-linear eigenproblem, which was solved by the continuation method.

On the basis of the obtained results, the dynamic characteristics of the entire structure, i.e. natural frequencies and non-dimensional damping ratios, were determined. These values were used to assess the impact of semi-rigid and viscoelastic connections on the dynamic response of the considered system.

By analyzing the selected frame structures, it was shown that the rotational elasticity of the joint has a large impact on the dynamic characteristics of the structure under consideration. It can be proved that when the rotational elasticity of the support is several times greater than the bending stiffness of the beam, the support can be treated as fully fixed. The proposed approach allows to obtain relatively accurate results with coarse discretization. Almost the same solutions were obtained when dividing each member into several finite elements and for a very fine division.

When examining the impact of the node damping parameter on the dynamic behavior of the structure, it was found that the increasing value of the damping coefficient does not change the resonant frequency, but it can significantly reduce the dynamic response of the structure for each mode of vibration. On the other hand, the influence of the parameter α describing the fractional model of the viscoelastic bond on the non-dimensional damping ratio of entire structure is monotonic, but the relationship is non-linear. In the considered frame, the viscoelastic rotational bonds in the nodes had the greatest impact on the damping of the second mode of vibration.

The results of calculations of selected structures with viscoelastic nodes confirm the effectiveness of the proposed approach.

Acknowledgements

The study has been supported by the University internal grant No. SBAD 0411/SBAD/0008. This support is gratefully acknowledged.

References

1. S.-H. CHOI, S.-E. KIM, *Optimal design of semi-rigid steel frames using practical, non-linear analysis*, Steel Structures, **6**, 141–152, 2006.
2. D. ANDERSON, F. BIJLAARD, D. NETHERCOT, *Analysis and Design of Steel Frames with Semi-rigid Joints*, ECCS, Technical Committee **8**, Structural Stability, 1992, doi: 10.5169/seals-50714.
3. S. ŽIVKOVIC, N. STOJKOVIĆ, M. SPASOJEVIĆ-ŠURDILOVIĆ, M. MILOŠEVIĆ, *Global analysis of steel constructions with semi-rigid connections*, Tehnički Vjesnik, **27**, 3, 951–960, 2020, doi: 10.17559/TV-20180414100627.
4. L. PINHEIRO, R.A.M. SILVEIRA, *Computational procedures for nonlinear analysis of frames with semi-rigid connections*, Latin American Journal of Solid and Structures, **2**, 339–367, 2005.
5. A.N.T. IHADDOUDÈNE, M. SAIDANI, M. CHEMROUK, *Mechanical model for analysis of steel frames with semi rigid joints*, Journal of Constructional Steel Research, **65**, 3, 631–640, 2009, doi: 10.1016/j.jcsr.2008.08.010.

6. M.H. ASL, B. FARIVAR, S.B. MOMENZADEH, *Investigation of the rigidity of welded shear tab connections*, Engineering Structures, **179**, 353–366, 2019, doi: 10.1016/j.engstruct.2018.10.077.
7. E. BAYO, J. GRACIA, *Stiffness modelling of 2D welded joints using metamodells based on mode shapes*, Journal of Constructional Steel Research, **156**, 242–251, 2019, doi: 10.1016/j.jcsr.2019.02.017.
8. S.B.M. BOUDIA, N. BOUMECHRA, A. BOUCHAIR, A. MISSOUM, *Modeling of bolted end plate beam-to-column joints with various stiffeners*, Journal of Constructional Steel Research, **167**, 105963, 2020, doi: 10.1016/j.jcsr.2020.105963.
9. L.M.C. SIMÕES, *Optimization of frames with semi-rigid connections*, Computers & Structures, **60**, 4, 531–539, 1996, doi: 10.1016/0045-7949(95)00427-0.
10. V.H. TRUONG, P.C. NGUYEN, S.E. KIM, *An efficient method for optimizing space steel frames with semi-rigid joints using practical advanced analysis and the micro-genetic algorithm*, Journal of Constructional Steel Research, **128**, 416–427, 2017, doi: 10.1016/j.jcsr.2016.09.013.
11. A.A. DEL SAVIO, D.A. NETHERCOT, P.C.G.S. VELLASCO, S.A.L. ANDRADE, L.F. MARTHA, *Generalized component-based model for semi-rigid beam-to-column connections including axial versus moment interaction*, Journal of Constructional Steel Research, **65**, 1876–1895, 2009, doi: 10.1016/j.jcsr.2009.02.011.
12. A. AHMED, *Prediction of moment-rotation characteristic of top- and seat-angle bolted connection incorporating prying action*, International Journal of Advanced Structural Engineering, **9**, 79–93, 2017, doi: 10.1007/s40091-017-0150-4.
13. A. ALHASAWI, S. GUEZOULI, M. COUCHAUX, *Component-based model versus stress-resultant plasticity modelling of bolted end-plate connection: Numerical implementation*, Structures, **11**, 164–177, 2017, doi: 10.1016/j.istruc.2017.05.004.
14. Y. HARADA, L.S. DA SILVA, *Three-dimensional macro-modeling of beam-to-rectangular hollow section column joints under cyclic loading. Part 1: Modeling of cycling out-of-plane behavior of single isolated plate element*, Journal of Constructional Steel Research, **162**, 105713, 2019, doi: 10.1016/j.jcsr.2019.105713.
15. P.C. NGUYEN, S.E. KIM, *Nonlinear inelastic time-history analysis of three-dimensional semi-rigid steel frames*, Journal of Constructional Steel Research, **101**, 192–206, 2014.
16. A.S. GALVÃO, A.R.D. SILVA, R.A.M. SILVEIRA, P.B. GONÇALVES, *Nonlinear dynamic behavior and instability of slender frames with semi-rigid connections*, International Journal of Mechanical Sciences, **52**, 12, 1547–1562, 2010, doi: 10.1016/j.ijmecsci.2010.07.002.
17. M. SEKULOVIC, R. SALATIC, M. NEFOVSKA, *Dynamic analysis of steel frames with flexible connections*, Computers & Structures, **80**, 11, 935–955, 2002, doi: 10.1016/S0045-7949(02)00058-5.
18. K. ZHU, F.G.A. AL-BERMANI, S. KITIPORNCHAI, B. LI, *Dynamic response of flexibly jointed frames*, Engineering Structures, **17**, 8, 575–580, 1995, doi: 10.1016/0141-0296(95)00008-U.
19. F. MINGHINI, N. TULLINI, F. LAUDIERO, *Vibration analysis of pultruded FRP frames with semi-rigid connections*, Engineering Structures, **32**, 10, 3344–3354, 2010, doi: 10.1016/j.engstruct.2010.07.008.

20. T. TÜRKER, M.E. KARTAL, A. BAYRAKTAR, M. MUVAFIK, *Assessment of semi-rigid connections in steel structures by modal testing*, Journal of Constructional Steel Research, **65**, 7, 1538–1547, 2009, doi: 10.1016/j.jcsr.2009.03.002.
21. A.U. ÖZTÜRK, M. SEÇER, *An investigation for semi-rigid frames by different connection models*, Mathematical and Computational Applications, **10**, 1, 35–44, 2005, doi: 10.3390/mca10010035.
22. S. GOPCEVIĆ, S. BRČIĆ, L. ŽUGIĆ, *Dynamic properties and time response of frameworks with semi-rigid and eccentric connections*, Architecture and Civil Engineering, **9**, 3, 379–393, 2011, doi: 10.2298/FUACE1103379G.
23. J. PAN, R. HUANG, J. XU, P. WANG, Z. WANG, J. CHEN, *Behavior of exposed column-base connections with four internal anchor bolts under seismic loading*, Structures, **34**, 105–119, 2021, doi: 10.1016/j.istruc.2021.07.016.
24. M. BAYAT, S.M. ZAHRAI, *Seismic performance of mid-rise steel frames with semi-rigid connections having different moment capacity*, Steel and Composite Structures, **25**, 1, 1–17, 2017, doi: 10.12989/scs.2017.25.1.001.
25. M. LATOUR, G. RIZZANO, *Mechanical modelling of exposed column base plate joints under cyclic loads*, Journal of Constructional Steel Research, **162**, 105726, 2019, doi: 10.1016/j.jcsr.2019.105726.
26. M. WANG, Y. SHI, Y. WANG, G. SHI, *Numerical study on seismic behaviors of steel frame end-plate connections*, Journal of Constructional Steel Research, **90**, 140–142, 2013, doi: 10.1016/j.jcsr.2013.07.033.
27. P.C. NGUYEN, S.E. KIM, *Second-order spread-of-plasticity approach for nonlinear time-history analysis of space semi-rigid steel frames*, Finite Elements in Analysis and Design, **105**, 1–15, 2015, doi: 10.1016/j.finel.2015.06.006.
28. H.K. CELİK, G. SAKAR, *Semi-rigid connections in steel structures: state-of-the-Art report on modelling, analysis and design*, Steel and Composite Structures, **45**, 1, 1–21, 2022, doi: 10.12989/scs.2022.45.1.001.
29. H.F. OZEL, A. SARITAS, T. TASBAHJI, *Consistent matrices for steel framed structured with semi-rigid connections accounting for shear deformation and rotary inertia effects*, Engineering Structures, **137**, 194–203, 2017, doi: 10.1016/j.engstruct.2017.01.070.
30. Z.J. FAN, J.H. LEE, K.H. KANG, K.J. KIM, *The forced vibration of a beam with viscoelastic boundary supports*, Journal of Sound and Vibration, **210**, 5, 673–682, 1998, doi: 10.1006/jsvi.1997.1353.
31. Y.L. XU, W.S. ZHANG, *Modal analysis and seismic response of steel frames with connection dampers*, Engineering Structures, **23**, 4, 385–396, 2001, doi: 10.1016/S0141-0296(00)00062-6.
32. A. BANISHEIKHOLESAMI, F. BEHNAMFAR, M. GHANDIL, *A beam-to-column connection with visco-elastic and hysteretic dampers for seismic damage control*, Journal of Constructional Steel Research, **117**, 185–195, 2016, doi: 10.1016/j.jcsr.2015.10.016.
33. Y.A. ROSSIKHIN, M.V. SHITIKOVA, *New method for solving dynamic problems of fractional derivative viscoelasticity*, International Journal of Engineering Science, **39**, 2, 149–176, 2001, doi: 10.1016/S0020-7225(00)00025-2.

-
34. R.M. LIN, T.Y. NG, *Development of a theoretical framework for vibration analysis of the class of problems described by fractional derivatives*, Mechanical Systems and Signal Processing, **116**, 78–96, 2019, doi: 10.1016/j.ymssp.2018.06.020.
 35. G. MUSCOLINO, A. PALMERI, A. RECUPERO, *Seismic analysis of steel frames with viscoelastic model of semi-rigid connections*, 13th World Conference on Earthquake Engineering, Vancouver, Canada, 2004.
 36. T. KOCATÜRK, Ö. TUNCER, M. SIMSEK, *Determination of steady response of portal frames with intermediate viscoelastic links*, International Journal of the Physical Science, **6**, 16, 3927–3937, 2011.
 37. S. KAWASHIMA, T. FUJIMOTO, *Vibration analysis of frames with semi-rigid connections*, Computers & Structures, **19**, 1-2, 85–92, 1984, doi: 10.1016/0045-7949(84)90206-2.
 38. Z. PAWLAK, R. LEWANDOWSKI, *The continuation method for the eigenvalue problem of structures with viscoelastic dampers*, Computers & Structures, **125**, 53–61, 2013, doi: 10.1016/j.compstruc.2013.04.021.
 39. R. LEWANDOWSKI, M. BAUM, *Dynamic characteristics of multilayered beams with viscoelastic layers described by the fractional Zener model*, Archive of Applied Mechanics, **85**, 12, 1793–1814, 2015, doi: 10.1007/s00419-015-1019-2.
 40. R. LEWANDOWSKI, P. LITEWKA, P. WIELENTEJCZYK, *Free vibrations of laminate plates with viscoelastic layers using the refined zig-zag theory, Part 1: Theoretical background*, Composite Structures, **278**, 114547, 2021, doi: 10.1016/j.compstruct.2021.114547.
 41. M. KAMIŃSKI, A. LENARTOWICZ, M. GUMINIAK, M. PRZYCHODZKI, *Selected problems of random free vibrations of rectangular thin plates with viscoelastic dampers*, Materials, **15**, 19, 6811, 2022, doi: 10.3390/ma15196811.
 42. R. LEWANDOWSKI, *Nonlinear steady state vibrations of beams made of the fractional Zener material using an exponential version of the harmonic balance method*, Meccanica, **57**, 2337–2354, 2022, doi: 10.1007/s11012-022-01576-8.
 43. A. CAPSONI, G.M. VIGANÒ, K. BANI-HANI, *On damping effects in Timoshenko beams*, International Journal of Mechanical Sciences, **73**, 27–39, 2013, doi: 10.1016/j.ijmecsci.2013.04.001.
 44. A.R.D. SILVA, E.A.P. BATELO, R.A.M. SILVEIRA, F.A. NEVES, P.B. GONÇALVES, *On the nonlinear transient analysis of planar steel frames with semi-rigid connections: from fundamentals to algorithms and numerical studies*, Latin American Journal of Solids and Structures, **15**, 3, 2018, doi: 10.1590/1679-78254087.

Received November 30, 2022; revised version April 6, 2023.

Published online June 15, 2023.
